Desalination and Water Treatment
www.deswater.com

doi:10.5004/dwt.2019.23766

153 (2019) 264–278
June

Photodestruction of Direct Yellow 11 in aqueous TiO_2 suspension: effect of operational parameters on detoxification, Langmuir–Hinshelwood kinetic expression and biodegradability

Sajjad Khezrianjoo

Department of Applied Chemistry, Malayer University, Malayer, 65719-95863, Iran, Tel./Fax +98 81 32355404, email: khezrianjoo@gmail.com (S. Khezrianjoo)

Received 23 June 2018; Accepted 8 January 2019

ABSTRACT

This study concerns the decolorization, dearomatization, mineralization and detoxification of the azo dye "Direct Yellow 11" using heterogeneous UV-TiO_2 process. Eco-toxicological evaluation was conducted using three-days of seed germination and root growth of dicotyledonous plant (*Lepidium sativum* L). Dependence of initial decolorization and mineralization rate on catalyst mass was investigated; meanwhile,hydroxyl radical portionin photocatalytic degradation of dyehas been evaluated in different catalyst concentrations. There was an unexpected increment in the toxicity of solution within the first 60 min of illumination. Although maximum decolorization and mineralization rates were obtained in alkaline pH, the highest detoxification rate was achieved in natural pH. In the pH values of 5, 6.8 and 9, adsorption constants in dark and photocatalytic degradation were determined; consequently, only at pH of 5 rate data was fitted correctly to the Langmuir–Hinshelwood kinetic model. Detoxification rate was increased slightly with the hoist of temperature and activation energy for photocatalytic decolorization and mineralization processes have been determined. Energy consumption was investigated in different dye concentrations and effective concentration (EC_{50}) of target dye was determined as 38.30 ± 0.79 (mg/L). Biodegradability of treated effluent of dye has also been investigated using ratio of biological oxygen demand to chemical oxygen demand (BOD_5/COD).

Keywords: Azo dye; Bioassay; Eco-toxicity; Energy consumption; Langmuir–Hinshelwood kinetic; Photocatalysis; Suspended reactor

1. Introduction

Textile industry produces nearly 10^8 ton of dyes annually in which azo dyes account for about 70% [1]. According to the estimates 2.8×10^5 tons of dyes are discharged into water sink; this is aesthetically undesirable and toxicity of these dyes caused death of the aquatic living species [2,3]. Meanwhile, azo dyes and their degradation products might be mutagenic and/or carcinogenic to microorganisms and humans [4]. Among the dye stuffs, basic, diazo and direct dyes showed the highest toxicity [5]. Dyes are mostly resistant to biodegradation and traditional physical methods do not result in effective degradation of them [3]. However, photocatalytic oxidation (PCO), especially using titanium dioxide (TiO_2) as catalyst, can deal constructively with the problem of dye destruction and several review articles deals with PCO of dyes using UV-TiO_2 process [5–7]. Whereas solar irradiation could be used as light source for PCO process, artificial light (UV lamp) is reported to be more efficient [8]. Meanwhile, due to the large surface area and efficient mass transfer in suspension or slurry systems, they are known as most effective reactor type for the PCO [6].

An important drawback of PCO process is that operational costs are relatively high and they often are too expensive to be applied as exclusive treatment [9]. Furthermore, due to the formation of resistant intermediates perfect mineralization of dye compound takes long time and it can be rarely achieved in an economically and environmental friendly way [10]. In order to make the PCO pro-

---

*Corresponding author.

1944-3994 / 1944-3986

cess more economic and efficient, several strategies such as application of UV-LED lamps or controlled periodic illumination (CPI) have been applied [11–13]. However, it is clear that with reduction of illumination time, energy consumption of PCO process can be reduced considerably. From the previous results it could be conclude that complete mineralization of dye compound it is not necessary; because the organic intermediate molecules which have been produced after some illumination are easily biodegradable and present very low toxicity values [14]. Furthermore, according to the Clean Water Act law, complete detoxification of polluted wastewaters could be considered as successful endpoint of treatment; this law prohibits the discharge of toxic pollutants in toxic amounts [15]. However, mechanism of PCO process is unpredictable and generated hydroxyl radicals in this process are non-selectively attack organic chemicals [11,16]. Therefore, various intermediates could be produced during the PCO of azo dyes and their toxicity play a crucial role in degradation process. It has frequently reported that, byproducts obtained by application of PCO processes show higher toxicity than the precursor dye compound [5,17,18]. Consequently, detection of intermediates and evolution of their toxicity during the PCO process is very important. Identification of the intermediates by modern analytical techniques (e.g. LC–UV/Vis, RP–HPLC, GC–MS and LC–MS) has been extensively studied by various authors and reviewed by Hisaindee et al. [19]. However, these methods are very costly and they are not widely available. Meanwhile, toxicity level of identified intermediates should be controlled afterwards [10]. However, toxicological behavior of unknown compounds could be successfully evaluated by direct toxicity testing systems [20]. Environmental Protection Agency (EPA) has also developed methods for estimating the toxicity of discharged wastewater and toxicological evaluation was included as suitable technique for regulating the quality of a permitted discharge [15]. To evaluate the detoxification of dyes several direct toxicity techniques have been developed and among them, seeds germinated and root growth of *Lepidium sativum* L. (*LS*L) plant were successfully used for toxicity testing of dye pollutants and their degradation byproducts [10,21]. This plant is repeatedly used to assess the eco-toxic risks from wastewater sources, river pollution, and industrially polluted soils [10]. *LS*L has advantage offered by some morphological and physiological properties (small size and high growth rate); meanwhile, it could grow in a wide range of pH values (3.5–10) [22].

Whereas effect of operational parameters is usually followed only by monitoring the decolorization and/or mineralization of target dye(s), in the main part of current work effect of catalyst concentration and solution pH on detoxification of dye polluted wastewater by PCO process has been studied. Degradation rate in different pH values was described based on the Langmuir–Hinshelwood (L–H) kinetic model and effect of catalyst concentration on hydroxyl radical generation was investigated. Activation energy for decolorization and mineralization processes was determined and toxicity reduction has been evaluated in various operating temperatures. Using different initial concentrations of dye electrical energy consumption and effective concentration (EC_{50}) have been evaluated and biodegradability of effluent was appraised based on (BOD_5/COD) and toxicity values.

2. Materials and methods

2.1. Reagents and reactor

Titanium dioxide (Degussa P25) catalyst provided by Degussa Company (Frankfurt, Germany) was used throughout this work without further modification. Its main physical data are BET surface area of 50 m^2/g and the average particle diameter of 30 nm, with about 80% anatase and 20% rutile structure [14]. The Direct Yellow 11 (DY11) azo dye $C_{16}H_{10}N_2Na_2O_7S_2$ (CI No: 40000, CAS No: 1325-37-7) was provided from AlvanSabet Company (Hamedan, Iran) with the purity of more than 98% (HPLC analysis). The molecular structure of this dye is shown in Fig. 1. Acidic or alkaline medium was obtained by addition of solutions of either hydrochloric acid or sodium hydroxide to the aqueous solutions containing the substrate; ethanol used to quench the hydroxyl radicals, were all Merck products. Distilled water was used to prepare the solutions.

A circulating up-flow annular and symmetric vertical Pyrex container with a conic body shape and capacity of about one liter was used as reactor. The UV lamp, Sunkun Co. Ltd. (Shenzhen, China), was mercury 250 W with 6.5 cm body length in the wavelength range of 280–400 nm and the maximum lamp emission of 365 nm measured by (TOPCON UV-R-1 spectroradiometer, Tokyo, Japan) was positioned centrally in the reactor and the quartz tube was used to hold the lamp. Details and schematic view of the constructed photo-reactor has been provided in Supplementary Information.

2.2. Experimental procedure

In this study initial DY11 concentration, in most cases, was set at 50 (mg/L) which was within the range of typical concentration in real textile wastewater [23,24]. For regulating the temperature, the reactor was equipped with a water-flow jacket (Fig. S1 – Supplementary Information); before each experiment one liter of dye solution was transferred to the reactor and external water flow with desire temperature (in most case 25°C) had circulated around the dye solution. When the desire internal temperature is reached, the pH of solution was adjusted using dilute NaOH or HCl solutions by means of a pH meter (Elico LI 127). Thereafter, known amount of TiO_2 (in most case 90 mg) was added to the dye solution and lamp was switched on. For evaluation of decolorization and mineralization of target dye samples (4 mL) were taken at 15 and 30 min intervals; after separation of the catalyst particles by centrifuging, decolorization analysis were performed with UV-Vis spectrophotometer (Systronics 168, Systronics India Limited, Delhi, India), measuring the absorbance at appropriate maximum wavelength (λ_{max}) at 404 nm in different pH values of 3, 5, 6.8 (natural), 9 and 11. Experiments were carried out at the isosbestic wave-

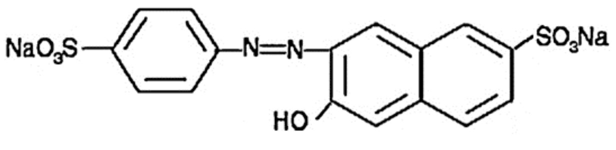

Fig. 1. Chemical structure of Direct Yellow 11 (DY11) azo dye.

length, but with increase in the pH the absorbance peak has been increased; hence, the appropriate calibration curves were used (Fig. S2 – Supplementary Information). To investigate the mineralization of dye, chemical oxygen demand (COD) was measured using a closed reflux digester reactor (HACH, DRB 200, Colorado, USA). Accordingly, after separation of catalyst, 2 ml of DY11 solution was added to the tubes containing potassium dichromate and sulfuric acid; these tubes with premeasured reagents are available commercially. The samples are then digested for 2 h at 150°C. During the digestion, almost all of the DY11 molecules are oxidized with the dichromate ($Cr_2O_7^{2-}$); this reaction reduces the dichromate ions to the chromium (Cr^{3+}). While the dichromate ions are visible at 400 nm, the chromium ions are at about 600 nm. Therefore, COD could be quantified by colorimetric determination using a spectrophotometer at 600 nm, which measures the light absorbance by the sample and correlates it to the COD value. The degradation efficiency or conversion (X%) of DY11 at any time was obtained by:

$$X\% = \frac{C_0 - C}{C_0} \times 100 \tag{1}$$

where C_0 is the concentration of DY11 before illumination and C is the concentration of DY11 after time t. According to Eq. (1), the COD reduction efficacy was also determined while C_0 is the initial COD value of DY11 and C is the COD value (mg O_2/L) at a given time (t). Dearomatization was monitored by (A/A_0) percentage, using peak intensity of DY11 solution in wavelength of around 250 nm, absorbance peak around this wavelength is attributed to the aromatic rings [25,26]; where A_0 is the initial measured absorbance and A is the peak intensity of treated solution at a given time.

2.3. Bioassay

Toxicity tests were carried out based on standard protocol [10]. The dicotyledonous garden cress *LS*L was used as indicator and seed germination as well as root measurement were conducted to evaluate the toxicity of DY11 and its degradation byproducts. The seeds were purchased from local market and all the seeds were examined and selected before the toxicity test under a magnifier (X5) meaning that seeds discolored, physically damaged or abnormally low were removed. While the pH of sample was 5, 6.8 (natural) or 9, a positive control was performed using sterile distilled water and the pH was adjusted to the desire values of 5, 6.8 (natural) or 9 with dilute hydrochloric acid or sodium hydroxide solutions. To determine the germination degree length of the main root was measured with a ruler against a black background. Samples were collected in 60 min intervals and catalyst particles were removed by centrifuging. Each sample was tested in an individual 10 cm Petri dish as container. Three layers of absorbent 9 cm round filter paper were placed at the bottom of the containers and seeds were evenly distributed and then 4 mL of sample were added to it. The containers were incubated for 72 h in a dark growth chamber at room temperature (25°C) and 90% relative humidity; the germination index (*GI*) was used to record the percentage of germination [21]:

$$GI\% = \left(\frac{S_S}{S_B}\right)\left(\frac{L_S}{L_B}\right) \times 100 \tag{2}$$

where S_S and S_B were the average number of germinated seeds for the sample and blank; L_S and L_B were the mean root length of seeds for the sample and blank, respectively. Fifteen seeds were distributed in each Petri dish and four replicate plates were used for each isolate; consequently, all the 60 obtained data have been analyzed by SPSS (Version 22.0) statistical package software for determination of *GI* using mean root length and average number of seeds germinated; standard division of these quantities was also calculated. One-way ANOVA was carried out to compare the means of different treatments as well as differences between individual means and control mean; when multiple regression analysis was performed using stepwise method and probability to F-enter = 0.05. It has been reported that the *GI* below the 40% indicates a high toxicity, value ranging from 40% to 60% represents the moderate toxicity and values more than 60% show the low toxicity [27,28].

The five-day biochemical oxygen demand assay (BOD_5) was carried out to evaluate the changes in biodegradability of the samples, according to the standard respirometric method [29], with a BOD system (VelpScientifica) and PolySeed® inoculum (Interlab®). The BOD_5 value was determined for DY11 with initial concentration of 50 mg/L and its degradation byproducts.

2.4. Dark surface adsorption

At the pH of 5, 6.8 and 91L of suspension containing of known concentration of dye (10–80 mg/L), in presence of catalyst (90 mg) was circulated in darkness for up to 45 min. Data obtained from the adsorption experiments was fitted to the modified empirical Langmuir equation [30]:

$$\frac{C}{Q} = \frac{1}{Q_{\max} K_{ads}} + \frac{C}{Q_{\max}} \tag{3}$$

where Q_{max} is the maximum absorbable dye quantity (mg/g) and K_{ads} is the equilibrium constant for adsorption (L/mg); the adsorbed quantity (Q in mg/g) was calculated as:

$$Q = \frac{V\Delta C}{m} \tag{4}$$

where ΔC is the difference between initial and equilibrium concentration (C_0 and C in mg/L), V is the solution volume (L), and m is the mass of TiO_2 (g). In order to find adsorption equilibrium time, samples were taken each 5 min and catalyst particles were removed by centrifuging.

2.5. Electrical energy per order of magnitude (E_{EO})

For the cases that are following the pseudo-first-order kinetic model, E_{EO} (kWh/m^3/order) is the number of electrical energy required to reduce the concentration of a pollutant by one order of magnitude (90%) in 1 m^3 of contaminated water in ideal batch reactors. E_{EO} has been accepted by the International Union of Pure and Applied Chemistry (IUPAC) and cost of treatment can be determined by this parameter. It can be calculated using the following formula [30,31]:

$$E_{EO} = \frac{1000 \times P \times t}{V \times 60 \times \log(C_0 / C)} \quad (5)$$

where P is the lamp power (kW), V is the treated volume (L), C_0 and C are the initial and final dye concentrations (mg/L) and t is the time of irradiation (min). When assuming the pseudo-first-order equation, the following can be applied:

$$\log\left(\frac{C_0}{C}\right) = 0.434 k_{obs} t \quad (6)$$

where k_{obs} is the pseudo-first-order rate constant (1/min) and t is the time of reaction (min). So, Eq. (5) can be transformed as simplified form of $\left(E_{EO} = \frac{38.4P}{Vk_{obs}}\right)$.

3. Results and discussion

3.1. The influence of catalyst loading

3.1.1. Effect of catalyst concentration on decolorization of DY11

The influence of catalyst concentration on PCO rate of DY11 with initial concentration of 50 mg/L in ambient temperature (25°C) and its natural pH 6.8 has been presented in Fig. 2. The reaction rate increased by raising the catalyst concentration (up to 90 mg/L); this could be due to the increase in active site of catalyst and generation of more hydroxyl radicals; meanwhile, more dye molecules can be adsorbed on catalyst surface. However, adding the higher amount of catalyst (more than 90 mg/L) can increase the opacity of suspension and decreases the reaction rate [32].

The relationship between the initial rate of PCO and catalyst concentration can be described as follows [30]:

$$r_0 \alpha [Catalyst]^n [dye] \quad (7)$$

As it can be seen in Fig. 3, dependence of the TiO_2 concentration on the initial decolorization rate of DY11 follows the similar relationship ($r_{Decolorization} \alpha [TiO_2]^{0.72}$), when the TiO_2 concentration is less than 90 mg/L.

While the most effective concentration of TiO_2 Degussa P-25, which is depends on reactor geometry and substrate nature, has been reported between 0.1–5.0 g/L [33], optimum concentration of catalyst in this investigation has been obtained as 90 mg/L. Using the same photo-reactor, very low optimum concentration of TiO_2 (≤ 0.1 g/L) was achieved in the previous works too [24,34–36]. Hence, this reactor is designed well to work with low concentration of catalyst; this could be accelerated the catalyst recovery stage and lower price should be spent for catalyst.

3.1.2. Effect of catalyst concentration on dearomatization, detoxification and mineralization

Effect of catalyst concentration (0, 30, 60 and 90 mg/L) on dearomatization, detoxification and mineralization processes has been also studied and results have been illustrated in Table 1. Dearomatization processes was monitored by measuring the peak intensity at about 250 nm. Mineralization process has been monitored by COD values and bioassay test was conducted in order to evaluate the toxicity of DY11 and its photodegradation byproducts using the *LS*L plant. These experiments were performed in ambient temperature (25°C) and natural pH (6.8). The initial concentration of DY11 was 50 mg/L and initiative COD and *GI* values for this solution were 46 mg O_2/L and 14%, respectively.

In the structure of azo dyes like DY11, the azo linkage (–N=N–) is particularly susceptible to electrophilic attack by hydroxyl radical [18]. Therefore, increase of the absorbance peak in the UV region (about 250 nm), in the first 60 min of the reaction, could be explained by the formation of the aromatic byproducts as a result of azo band cleavage. However, no increase of the absorbance in the UV region was observed during the decolorization of some azo dyes; adsorption of the generated byproducts on catalyst surface has been reported to be the main reason of this observation

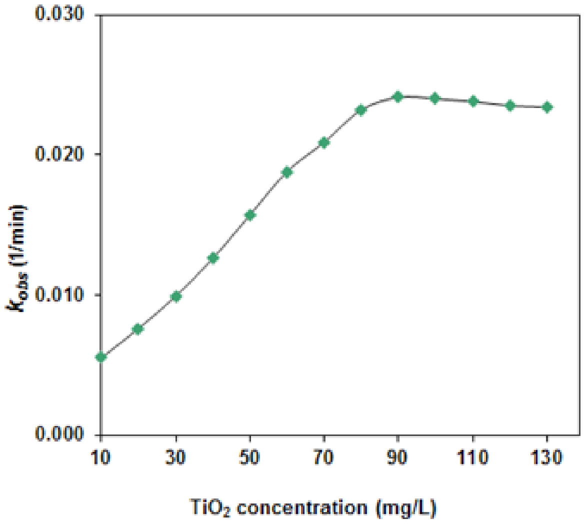

Fig 2. Effect of the amount of TiO_2 on PCO rate constant; $[DY11]_0$ = 50 (mg/L), T = 25°C and pH = 6.8 (natural).

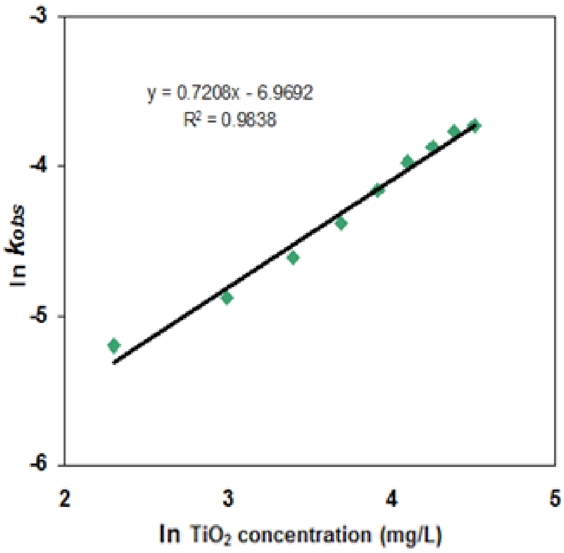

Fig. 3. Relationship between ln(k_{obs}) and ln(TiO_2 mass); $[DY11]_0$ = 50 (mg/L), T = 25°C and pH = 6.8 (natural).

Table 1
Effect of catalyst concentration on mineralization, detoxification and dearomatization of DY11 during the photodestruction process; $[DY11]_0$ = 50 (mg/L), T = 25°C and pH = 6.8 (natural)

Reaction time (min)	COD removal%				*GI*%				(A/A_0)% about 250 nm			
	TiO_2 mass (mg/L)				TiO_2 mass (mg/L)				TiO_2 mass (mg/L)			
	0	30	60	90	0	30	60	90	0	30	60	90
60	5	18	23	37	23	12	11	8	91	109	118	131
120	8	34	48	64	34	38	49	59	85	71	53	37
180	11	45	64	78	49a	62	78	93a	76	60	37	9
240	12	54	75	86	53a	84a	91a	98a	72	49	15	3
300	14	64	84	91	56a	90a	97a	100a	69	38	8	0

Values followed by the same letter within the same column do not differ significantly from each other at the 5% level of probability.

[18]. In the current study, the concentration of catalyst was low; thus, the adsorption sites on catalyst surface is limited and low tendency of generated intermediated could be adsorbed. Therefore, UV$_{250}$ peak intensity has been increased in early moments of illumination. The UV-Vis spectra analysis as well as image of germination and root growth of *LS*L during the PCO process can be found in the Supplementary Information. Although the obtained data from current work does not allow the precise identification of generated intermediate, the major intermediates which could be generated during the PCO of azo dyes are reported to be substituted phenols, aromatic hydroxyl amines and nitroso compounds [7]. The aromatic amines which could be produced by oxidative cleavage of the azo bond are considered as hazardous substances and the use of azo dyes which, by reductive cleavage, may release certain amines at concentrations more than 30 mg/L has prohibited by European Commission [37].

As it can be seen in Table 1, during the PCO of DY11 dearomatization and detoxification trends are in reasonably good agreement. In the first 60 min of irradiation, the obtained spectra show the increase in absorbance peaks at about 250 nm; meanwhile, the toxicity of the solution was also increased in this period. With increase in the catalyst mass, in first 60 min of irradiation, the number and/or concentration of toxic intermediates have been increased too. For illumination times longer than 60 min, absorbance peaks at around 250 nm and solution toxicity tended to decrease and with increasing in catalyst mass these trends were accelerated.

While for illumination times longer than 180 min higher detoxification and mineralization can be expected for the PCO process, for the case of photolysis (no catalyst) these changes were not considerable. COD and *GI* values as well as absorbance peaks at around 250 nm have been decreased modestly in the first 180 min of irradiation and approximately leveled off after this time; this could be due to the formation of stable intermediates which are not more degradable by photolysis process. Thus, presence of catalyst is essential for an effective detoxification and mineralization of DY11. The COD removal rate of DY11 using catalyst concentrations of 30, 50, 60 and 90 mg/L have been expressed by the pseudo-first-order kinetic model and the related rate constants were calculated as 3.3×10^{-3}, 4.8×10^{-3}, $5.9\times 10^{-3}$and 8.2×10^{-3} 1/min, respectively. As it can be seen in Fig. 4, the relationship between the initial rate of DY11 mineralization and TiO_2 concentration,according to Eq. (7), was determined as ($r_{Mineralization} \alpha [TiO_2]^{0.83}$).

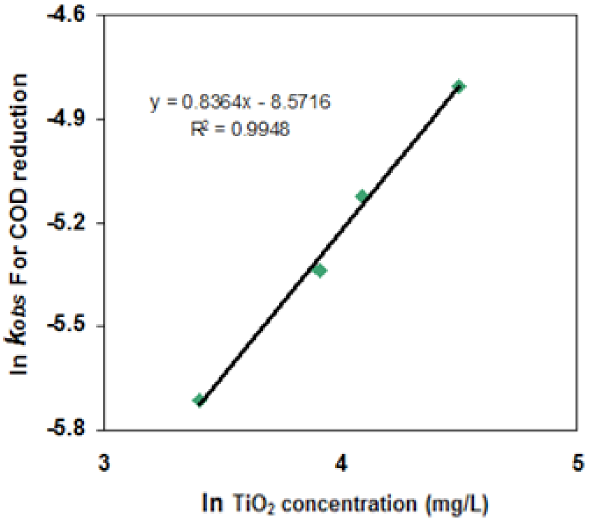

Fig. 4. Relationship between ln(k_{obs}) (for COD reduction) and ln (TiO_2mass); $[DY11]_0$ = 50 (mg/L), T = 25°C and pH = 6.8 (natural).

Therefore, compare to the decolorization process, mineralization of DY11 was more dependent on the catalyst concentration. The obtained data indicate that, optimum catalyst concentration for decolorization of DY11 (90 mg/L) shows the highest efficiency in the detoxification and mineralization processes too. Using the optimum catalyst concentration, 0.75 kWh energy was consumed to reach the nearly complete detoxification (*GI* = 93%); while in this stage only 78% of dye was mineralized and to reach the almost complete mineralization (94% COD reduction), 1.5 kWh energy was required.

3.2. Investigation on active species

In some of previous researches the PCO was constituted into two paths only: (1) bulk degradation by hydroxyl radicals (•OH) and (2) degradation of pollution by positive holes during the adsorption on catalyst surface [24,30]. In order to evaluate these two paths, experiments have been conducted by adding the radical scavenger (e.g. ethanol) to the solution. Consequently, obtained data was used to calculate the contribution of hydroxyl radicals and/or electron-hole portion. However, recent researches indicate that main active species in the PCO process are holes, electrons, •OH and $O^{2\bullet-}$; meanwhile, contribution of these species should be measured exclusively [38,39].

To study the role of •OH species, experiments were performed, with different amounts of added ethanol as radical scavenger [35]. Consequently,the contribution •OH in degradation process using catalyst concentrations of 30, 60 and 90 mg/L at different times are determined and illustrated in Fig. 5. Further background information can be found in the Supplementary Information.

With increase in reaction time and catalyst concentration the portion of •OH in dye degradation increased too. In Fig. 5, the written number on each column represents the percentage of oxidize dye via •OH; for instance, using catalyst concentration of 90 mg/L after 30 min of illumination totally 55% of DY11 was degraded and from this amount 22% was oxidized by•OH; consequently, almost 40% of total degradation in this time was accomplished by •OH. Dye degradation via hydroxyl radicals has been enhanced by increase in catalyst concentration and reaction time. With increase in catalyst concentration more active site would be available in the suspension; so, more hydroxyl radicals could be generated. Meanwhile, the average distance of molecular diffusion of hydroxyl radicals depends on the nature and concentration of the adsorbed substrate [40,41]. During the illumination several intermediates could be produced and adsorbed on the TiO_2; hence, a part of catalyst surface engages on interaction with them. The enhancement in •OH portion during the reaction could be due to this phenomenon.

3.3. Effect of pH

3.3.1. Effect of pH on surface adsorption and decolorization of DY11

For studying the adsorption of DY11 on catalyst surface in the initial pH values of 3, 5, 6.8, 9 and 11, solution containing 50 mg/L of dye and 90 mg/L of catalyst, has been circulated in absence of UV light for up to 45 min in ambient temperature and percentage of dye adsorption on catalyst surface was determined; results are presented in Table 2. The point of zero charge (P_{ZC}), for TiO_2 (Degussa P25), in water is around pH 6.8 [32]; therefore, at acidic pH, the particle surface is positively charged, while at pH > 6.8, it is negatively charged. Generally, predictable trend of DY11 adsorption on catalyst surface has been observed; at pH of 5, electrostatic attraction between positively charged TiO_2 surface and negatively charged sulfonic group leaded to strong adsorption. Lowering of the pH of the solution (pH = 3) makes the TiO_2 particles aggregated; hence, dye adsorption value was reduced slightly. At the initial pH of 9 and 11, TiO_2 surface becomes negatively charged and low tendency to be adsorbed due to electrostatic repulsion between the dye sulfonic groups and catalyst surface.

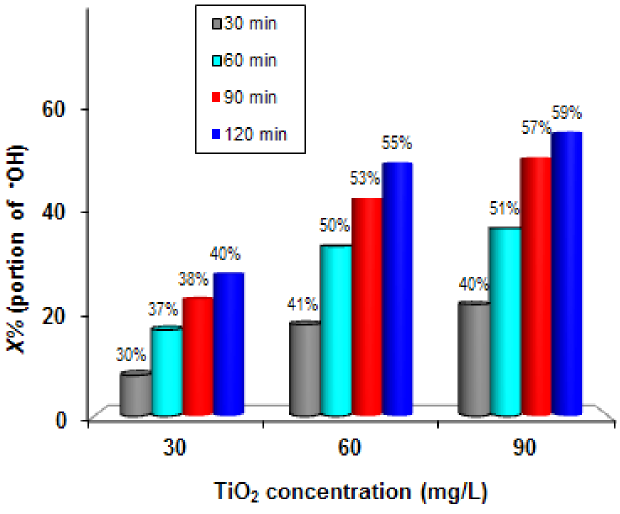

Fig. 5. The contribution of hydroxyl radical in degradation of DY11 by different catalyst concentrations; $[DY11]_0$ = 50 (mg/L), T = 25°C and pH = 6.8 (natural).

The effect of pH on the PCO of DY11 has also been studied at same range of pH 3–11. As it can be seen in Table 2, pH plays an important role in the PCO of DY11. At acidic initial pH of 3 and 5, relatively low rate constants were obtained, while the rate constant has been enhanced in alkaline medium. The obtained data in this work are in agreement with the previous reported results [7]. In alkaline solution, by oxidizing the hydroxide ions available on TiO_2 surface more hydroxyl radicals could be generated, so the efficiency of the PCO process is logically enhances [7]. However, the hydroxyl radicals could be rapidly scavenged at high pH values (pH = 11) that reduce the PCO rate [32]. On the other hand, agglomeration of TiO_2 particles in the acidic condition can reduce the dye adsorption and PCO efficiency [32].

3.3.1. Effect of pH on dearomatization, detoxification and mineralization of DY11

Although, the dicolorization of dye polluted wastewaters can be an important achievement for the PCO process; but, the main propose of this process is the mineralization and reduction of the toxic properties of the target pollutions. Consequently, efficiency of mineralization and detoxification processes were evaluated in acidic and alkaline mediums (initial pH values of 5 and 9); dearomatization of dye was also followed by monitoring the absorbance peaks at around 250 nm (UV_{250}) and results have been shown in Table 3 (related data to the natural pH (6.8) can be found in Table 1). Data indicate that, after nearly complete decolorization (90%) of DY11 with initial concentration of 50 mg/L in presence of TiO_2 (90 mg/L) in the pH values of 5, 6.8 and 9 solution not mineralized yet and had toxic properties.

In pH of 9, during the first 60 min of reaction, toxicity and UV_{250} wavelength absorbance peak was increased faster than natural pH. Meanwhile, despite the decoloriza-

Table 2
Adsorption of DY11 on catalyst surface and PCO rate constant in different initial pH values; $[DY11]_0$ = 50 (mg/L), $[TiO_2]$ = 90 (mg/L) and T = 25°C.

pH	3	5	6.8	9	11
Dark adsorption% (after 45 min)	1.53	1.58	1.41	0.38	0.32
$k_{obs} \times 10^2$ (1/min)	1.80	1.92	2.41	2.97	2.60

Table 3
Effect of initial pH values on mineralization, dearomatization and detoxification of DY11 during the PCO processes; $[DY11]_0$ = 50 (mg/L), $[TiO_2]$ = 90 (mg/L) and T = 25°C

Reaction time (min)	COD removal%		*GI*%		UV_{250} (A/A_0)%	
	Initial pH		Initial pH		Initial pH	
	5	9	5	9	5	9
60	33	38	23	5	87	144
120	57	67	55	51	45	42
180	71	81	81	80	23	17
240	79	89	96a	94a	12	6
300	87	94	100a	100a	4	0

Values followed by the same letter within the same column do not differ significantly from each other at the 5% level of probability

tion and mineralization rate in alkaline pH was higher than natural pH, more energy has been consumed for nearly complete detoxification of dye. Thus, in alkaline medium more number and/or concentration of toxic intermediates have been generated and remained in solution than natural pH. Generally, the relationship between the detoxification and the UV_{250} removal trend show that the prerequisite of complete detoxification was a striking reduction (nearly perfect removal) in aromaticity. Consequently, peak intensity at UV_{250} that was closely related with the toxicity reduction could be considered as the control parameter for the detoxification of the tested compound. The obtained data in the current work are in good agreement with the previous reported results[25,26]. In pH 9, the required energy for almost complete detoxification (*GI* = 94%) was determined to be 1.0 kWh and in this stage near to 89% of dye has been mineralized. In the pH of 5, no increase was observed in solution toxicity as well as absorbance peaks at around 250 nm. As it has been described hydroxyl radicals play an important role in PCO of DY11; at low pH the hydrogen ions interact with azo linkage and decrease the electron densities at azo group. Consequently, the reactivity of hydroxyl radical by electrophilic mechanism decreases and the azo band cleavage reduces [7]. Thus, less aromatic intermediates could be formed in acidic medium. Meanwhile, the generated intermediates could be adsorbed on positively charged catalyst surface. To reach the almost complete detoxification (*GI* = 96%) in the pH of 5, nearly 1.0 kW h energy was consumed and 79%of dye was mineralized in this stage. Dissimilar toxicity reduction and mineralization rate in the examined pH values can be attributed to the generation of different type and/or concentration of intermediates in those mediums. Meanwhile, pH of solution can affect the adsorption of generated intermediates on catalyst surface.

3.4. Effect of temperature

The effect of temperature on decolorization rate, dark surface adsorption, toxicity reduction and mineralization rate of target dye has been studied. The PCO of dye, with initial concentration of 50 mg/L, was carried out in natural pH and catalyst concentration of 90 mg/L. Although increase in temperature goes against the adsorption of DY11 on the catalyst surface, PCO decolorization and mineralization rate was increased with the hoist of temperature (Table 4).

Table 4
Effect of temperature on decolorization and mineralization rate as well as dark surface adsorption of DY11; $[DY11]_0$ = 50 (mg/L), $[TiO_2]$ = 90 (mg/L) and pH = 6.8 (natural)

Temperature (°C)	5	15	25	35	45
Dark adsorption% (after 30 min)	1.48	1.45	1.41	1.38	1.34
$k_{obs} \times 10^2$ (1/min) for Decolorization	2.02	2.25	2.41	2.57	2.82
$k_{obs} \times 10^2$ (1/min) for Mineralization	0.69	0.74	0.82	0.86	0.93

According to the obtained data (Fig. 6), the apparent activation energy (E_a), using Arrhenius equation [30], for the PCO decolorization and mineralization of DY11 has been calculated to be 5.89 and 5.50 kJ/mol; this apparent energy represents the total activation energy of adsorption and PCO of DY11. Since, the band-gap energy of TiO_2 is too high to be overcome by thermal activation energy; usually, the UV/TiO_2 reaction is not very dependent on temperature [42]. However, it has been reported that PCO could be highly temperature sensitive [43].

To investigate the influence of reaction temperature on solution toxicity, the *GI* values were measured in all the examined temperatures (Fig. 7). In the first 60 min of PCO processes, toxicity of treated solution increased leisurely with rise in temperature and after this time detoxification rate increased with the hoist of temperature.

3.5. Kinetic studies

The effect of various initial DY11 concentrations on the PCO rate at pH of 5, 6.8 and 9 in the presence of TiO_2 90 mg/L have been investigated; the obtained rate constants are listed in Table S1 – Supplementary Information. Consequently, the experimental data have been rationalized in terms of the L–H kinetic model [30], to describe the solid-liquid reaction:

$$\frac{1}{k_{obs}} = \frac{1}{k_c K_{LH}} + \frac{[DY11]_0}{k_c} \tag{8}$$

where k_{obs} (1/min) is the pseudo-first-order rate constant, K_{LH} (L/mg) is the L–H adsorption equilibrium constant and k_c (mg/L min) is the kinetic rate constant of surface reaction. According to Fig. 8, using a least square best fitting procedure (while initial DY11 concentration was less than 50 mg/L), for the examined pH values of 5, 6.8 and 9, k_c were determined as 1.107, 1.257 and 1.562 mg/L min; K_{LH} were also calculated as 0.150, 0.387 and 1.124 L/mg, respectively.

Although, in many studies, L–H kinetic model has been described using the rate of PCO reaction with various concentrations of a target substrate [32,34,43], the use of the dark adsorption measurement is required; if the kinetically adsorption equilibrium constant is different from that of

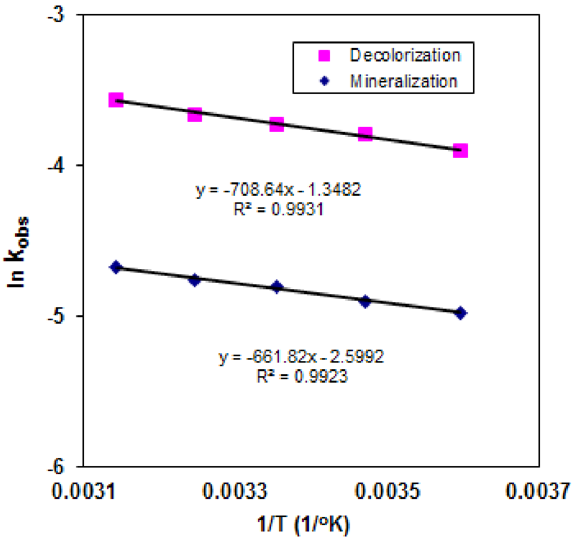

Fig. 6. Linear variation of ln(k_{obs}) versus 1/T for decolorization and mineralization of DY11 by PCO process; $[DY11]_0 = 50$ (mg/L), $[TiO_2] = 90$ (mg/L) and pH = 6.8 (natural).

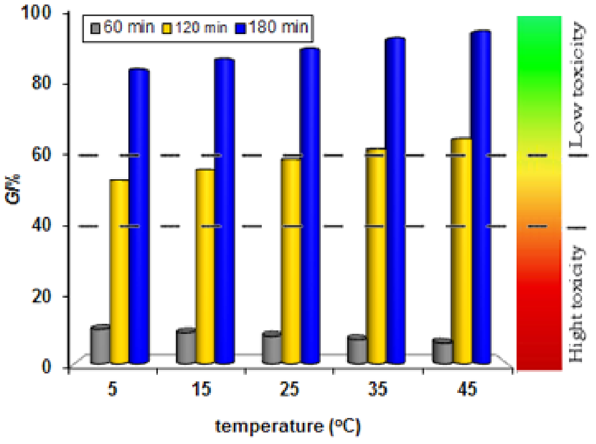

Fig. 7. Influence of reaction temperature on detoxification of DY11 in PCO process; $[DY11]_0 = 50$ (mg/L), $[TiO_2] = 90$ (mg/L) and pH = 6.8 (natural).

obtained in dark, the L–H kinetic model cannot be adopted [30]. In order to obtain the adsorption equilibrium constant, the influence of the different initial concentrations of DY11 on the surface adsorption at pH of 5, 6.8 and 9 have been studied; details are available in the Supplementary Information. According to Eq. (3), while initial concentration of DY11 was below than 50 mg/L, data obtained from the adsorption experiments was fitted to the Langmuir equation (Fig. 9).

Accordingly, Langmuir adsorption constant (K_{ads}) for the examined pH values of 5, 6.8 and 9 were determined to be 0.148, 0.179 and 0.134 L/mg. The maximum absorbable dye quantities (Q_{max}) were also calculated as 9.94, 8.57 and 2.39 mg/g, for initial pH values of 5, 6.8 and 9, respectively. The adsorption–desorption equilibrium of DY11 over both of catalysts surface occurred in relatively short time

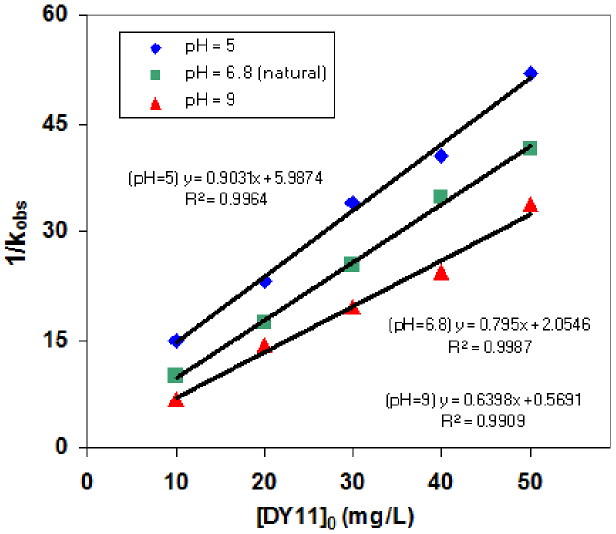

Fig. 8. Variation of reciprocal of constant rate versus different initial concentrations of DY11 in different pH values; $[DY11]_0 = 50$ (mg/L), $[TiO_2] = 90$ (mg/L) and T = 25 (°C).

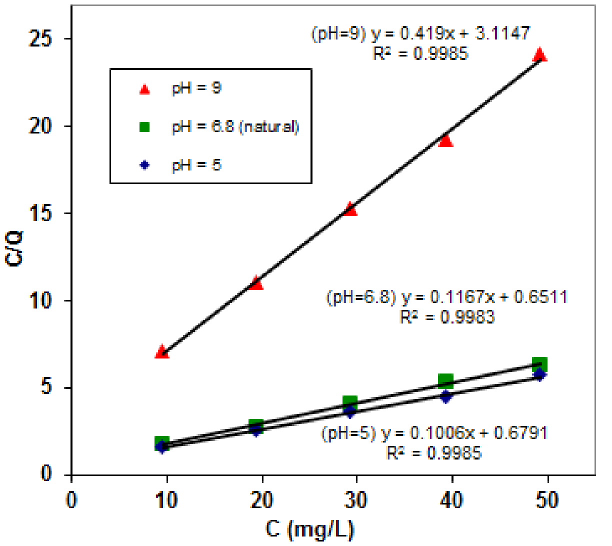

Fig. 9. Determination of the Langmuir equilibrium constant (K_{ads}) and maximum absorbable dye quantity (Q_{max}) of DY11 in presence of TiO_2 in different pH values; $[TiO_2] = 90$ (mg/L) and T = 25 (°C).

period. It has been reported that the adsorption process in a concise time could be described by film diffusion model [44]. DY11 adsorption at the initial pH values of 5, 6.8 and 9 was occurred within approximately 15, 20 and 30 min over the TiO_2 catalyst surface. These observations indicate that with increase in the Q_{max} dye adsorption equilibrium time decreases. In pH values of 6.8 and 9, adsorption constant in the kinetic model were determined to be higher from that of obtained in dark. Since the adsorptive sites on the TiO_2 surface could be changed as result of UV illumination and the amount of these sites would be scarce to start the reaction, adsorption constant in the kinetic model may be determined contrary to that of obtained in dark. Meanwhile, the observation of $K_{LH} > K_L$ suggests that reaction takes place not only at the surface of catalyst, but also in the bulk solution [45]. At pH of 5 adsorption constant in kinetic model was found to be close to that of obtained in the dark ($K_{LH} = 1.01\ K_{ads}$); thus, PCO of DY11 at this pH satisfactorily follows the L–H kinetic model.

3.6. Biodegradability tendency

Biodegradability of treated effluent of DY11 with initial concentration of 50 mg/L in presence of TiO_2 (90 mg/L), ambient temperature and natural pH by PCO process has also been studied. Generally, the wastewaters that have considerable toxicity to enzymes, microorganisms and cells could not be considered as readily biodegradable. Nevertheless, another straight way to quantify the biodegradability of polluted wastewater is via (BOD_5/COD) ratio [46]. When (BOD_5/COD) parameter, which is known as "biodegradability index" (*BI*), is higher than 0.4 wastewater is biodegradable and the value of 0.3 to 0.4 shows that wastewater is partially biodegradable [46]. Before PCO, the *GI* and *BI* values (14% and 0.09) clearly demonstrate that DY11 with initial concentration of 50 mg/L is not biodegradable. Despite after almost complete decolorization (after about 90 min of irradiation and about 90% decolorization) *GI* value of 36% indicated that treated solution is still highly toxic, obtained *BI* (0.43) demonstrated that effluent is biodegradable. However, after about 120 min of irradiation *GI* was reached to 59% which is represents the approximately low toxicity; in this time *BI* were obtained to be 0.66. Therefore, after about 120 min of illumination, more confidently can decide to stop the PCO and continue the mineralization with biological treatment producers.

3.7. Evaluation of E_{EO} and EC_{50} by different initial dye concentration

Toxicity data could be represented as a concentration causing a specific effect such as death or growth inhabitation in 50% of the tested organisms (effective concentration, EC_{50}). In order to obtain this eco-toxicological indicator (EC_{50}), effect of different concentrations of DY11 (10, 20, 30, 40 and 50 mg/L) that induce inhibition on *LSL* root growth (Fig. 10) and seed germination percentage (Fig. 11) have been studied and $EC_{50}$was calculated from the data of a concentration response line by using the right-angled triangle principles [47]. Consequently, concentration of DY11 that indicated EC_{50} was determined to be 38.30 ± 0.79 mg/L. The image of germination and root growth of *LSL* in different concentrations of DY11 can be found in the Fig. S7 – Supplementary Information.

The initial concentration of the DY11 has a fundamental effect on the degradation rate, i.e. degradation rate constant decreased with increase in the DY11 initial concentration. Meanwhile, the reaction rate constant can determine the quantity of E_{EO}. Accordingly, the evolution of energy consumption for PCO of DY11 in presence of TiO_2 (90 mg) at natural pH and ambient temperature as a function of initial dye concentration has been presented in Fig. 12. As it can be seen, the relationship between the E_{EO} and the initial con-

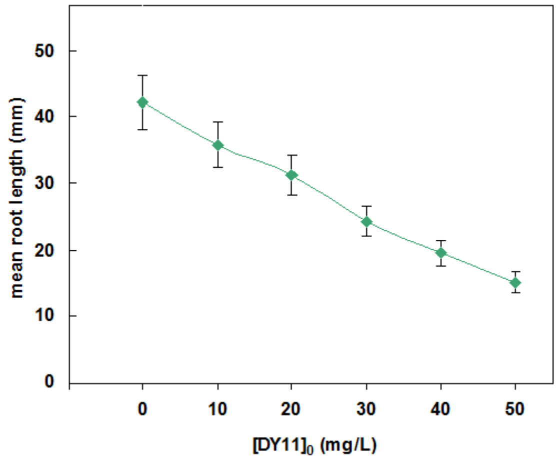

Fig. 10. Influence of DY11 concentration on root length of *LSL*; T = 25 (°C) and pH = 6.8 (natural).

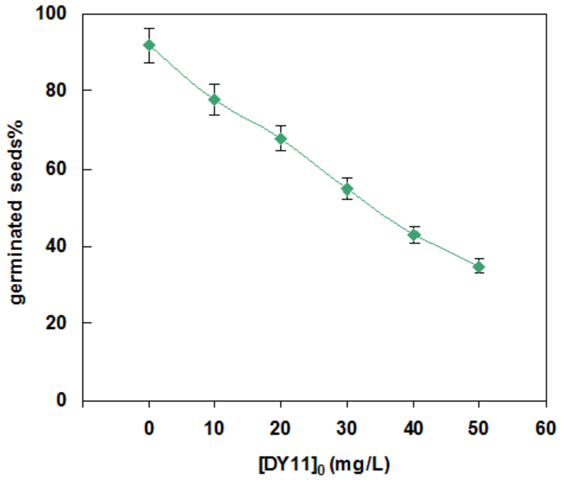

Fig. 11. Influence of DY11 concentration on the germination of *LSL* seeds; T = 25 (°C) and pH = 6.8 (natural).

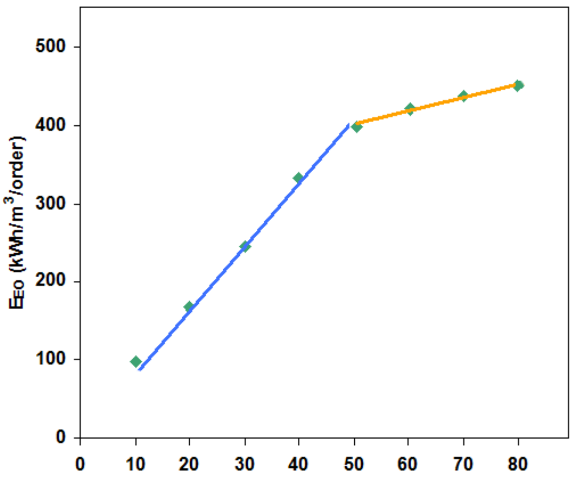

Fig. 12. Evolution of energy consumption for PCO of DY11 as a function of initial dye concentration; [TiO_2] = 90 (mg/L), T = 25 (°C) and pH = 6.8 (natural).

centration of dye until 50 mg/L can be written as $E_{EO}\alpha$ 8.18 $[DY11]_0$; beyond this concentration this relationship was changed to $E_{EO}\alpha$ 1.55 $[DY11]_0$. Since, the electrical energy price in US market was 0.068 US$/kWh in 2015 [31], cost of decolorization for one cubic meter of DY11 with initial concentrations of 30, 50 and 80 mg/L could be determined as 16.52, 27.08 and 30.36 US$.

Generally with increase in the dye concentration PCO efficiency has been reduced and more energy was required for degradation of DY11. As it has been explained, with increase in concentration of DY11, more dye molecules can get adsorbed on the catalyst surface and requirement of reactive species needed for the degradation of dye increases too. However, the photogenerated electron-holes and formation of hydroxyl radicals on the catalyst surface remains constant for a given catalyst concentration and light intensity. Therefore, the available $^{\bullet}$OH and electron/holes were inadequate for the dye degradation at higher concentration. In addition, enhancement in DY11 concentration can lead to the formation of more intermediates, which can be adsorbed on catalyst surface. Slow diffusion of the formatted intermediates from the surface of catalyst can result in the deactivation of active sites of the catalyst; meanwhile, the active sties of catalyst surface would be occupied by the adsorbed reactant molecules. Hence, degradation rate reduces with increase in dye concentration and more energy is required for dye degradation.

According to the obtained data in the current work, after 120 min of PCO, treatment process could be continued by biological methods. However, for nearly complete detoxification (*GI* = 93%) and mineralization (94% COD reduction), PCO process should be continued for more 60 and 240 min. Consequently, for almost complete detoxification and mineralization of 15.5×10^6 m^3 of this effluent, equal to the 1% of annual India's textile industry wastewater production [48], approximately more 2.60×10^5 and 1.04×10^6 US$ should be spent for electricity bill. Consequently, continuation of the treatment without bioassay evaluation is not economical and monitoring of effluent biodegradability before reaching complete mineralization is more than justified.

4. Conclusions

Heterogeneous photocatalytic degradation process, with commercially available nano TiO_2 photocatalyst (Degussa P25) in slurry reactor, was successfully applied for the treatment of azo dye DY11 in aqueous suspension. The core findings of this research can be summarized as followings:

- Using the moderate photoreactor very low optimum concentration of suspended catalyst (90 mg/L) was obtained.
- The mineralization of dye was depended more than decolorization to the catalyst mass.
- In first 60 min of irradiation, the number and/or concentration of toxic intermediates were increased and for illumination times longer than 60 min toxicity tended to decrease; with increasing in catalyst mass these trends were accelerated.
- With increase in reaction time and catalyst concentration the contribution of hydroxyl radicals in dye degradation have been increased.
- Decolorization and mineralization cannot be easily correlated to toxicity. While maximum rate of decolorization and mineralization was obtained in pH of 9; highest rate of detoxification was achieved in natural pH 6.8.
- Although in pH values of 6.8 and 9 toxicity was increased in first 60 min of irradiation, no increase was observed in solution toxicity in pH of 5.
- Activation energy (E_a) for decolorization and mineralization processes was determined as 5.89 and 5.50 kJ/mol and detoxification efficiency was increased modestly with the hoist of temperature.
- Dearomatization of DY11 during the PCO could be considered as a control parameter for its detoxification.
- Only at the pH of 5 the rate data was fitted correctly to the L–H kinetic model.
- Germination index (*GI* = 14%) and biodegradability index (*BI* = 0.09) indicates that DY11 with initial concentration of 50 mg/L is toxic and non-biodegradable.
- The effective concentration (EC_{50}) of DY11 was obtained to be 38.30 ± 0.79 mg/L.
- Despite after 90% of decolorization *GI* indicated that treated solution is still highly toxic, obtained *BI* demonstrated that effluent is biodegradable; thus, the end time of PCO should be determined more carefully.
- The relationship between the E_{EO} and initial concentration of dye until 50 mg/L has been determined as E_{EO} α 8.18 $[DY11]_0$; beyond this concentration this relationship was changed to E_{EO} α 1.55 $[DY11]_0$.
- Continuation of the photocatalytic degradation without bioassay evaluation was not economical.

Acknowledgement

I wish to thank Prof. M. Khanjani at the Faculty of Agriculture, University of Bu-Ali Sina, for his assistance in carrying out the experiments for toxicity investigations. I am also grateful to Mrs. M. Mohammadi for assistance with statistical analysis.

References

[1] H. Lade, S. Govindwar, D. Paul, Mineralization and detoxification of the carcinogenic azo dye Congo Red and real textile effluent by a polyurethane foam immobilized microbial consortium in an upflow column bioreactor, Int. J. Environ. Res. Public Health, 12 (2015) 6894–6918.

[2] A. Asghar, A.A.A. Raman, W.M.A.W. Daud, Recent advances, challenges and prospects of in situ production of hydrogen peroxide for textile wastewater treatment in microbial fuel cells, J. Chem. Technol. Biotechnol., 89 (2014) 1466–1480.

[3] M. Eskandarian, F. Mahdizadeh, L. Ghalamchi, S. Naghavi, Bio-Fenton process for Acid Blue 113 textile azo dye decolorization: characteristics and neural network modeling, Desal. Water Treat., 52 (2014) 4990–4998.

[4] D. Daâssi, H. Zouari-Mechichi, F. Frikha, M.J. Martinez, M. Nasri, T. Mechichi, Decolorization of the azo dye Acid Orange 51 by laccase produced in solid culture of a newly isolated trametes trogii strain, 3 Biotech, 3 (2013) 115–125.

[5] A. Ajmal, I. Majeed, R.N. Malik, H. Idriss, M.A. Nadeem, Principles and mechanisms of photocatalytic dye degradation on TiO_2 based photocatalysts: a comparative overview, RSC Adv., 4 (2014) 37003–37026.

[6] M.N. Chong, B. Jin, C.W.K. Chow, C. Saint, Recent developments in photocatalytic water treatment technology: a review, Water Res., 44 (2010) 2997–3027.

[7] M.A. Rauf, M.A. Meetani, S. Hisaindee, An overview on the photocatalytic degradation of azo dyes in the presence of TiO_2 doped with selective transition metals, Desalination, 276 (2011) 13–27.

[8] T.E Agustina, R. Komala, M. Faizal, Application of TiO_2 nano particles photocatalyst to degrade synthetic dye wastewater under solar irradiation, Contemp. Eng. Sci., 8 (2015) 1625–1636.

[9] J. García-Montaño, X. Domènech, J.A. García-Hortal, F. Torrades, J. Peral, The testing of several biological and chemical coupled treatments for Cibacron Red FN-R azo dye removal, J. Hazard. Mater., 154 (2008) 484–490.

[10] L.C. Apostol, C. Smaranda, M. Diaconu, M. Gavrilescu, Preliminary ecotoxicological evaluation of Erythrosin B and its photocatalytic degradation products, Environ. Eng. Manage. J., 14 (2015) 465–471.

[11] M.R. Eskandarian, H. Choi, M. Fazli, M.H. Rasoulifard, Effect of UV-LED wavelengths on direct photolytic and TiO_2 photocatalytic degradation of emerging contaminants in water, Chem. Eng. J., 300 (2016) 414–422.

[12] O. Tokode, R. Prabhu, L.A. Lawton, P.K.J. Robertson, Controlled periodic illumination in semiconductor photocatalysis, J. Photochem. Photobiol. A, 319–320 (2016) 96–106.

[13] M. Rasoulifard, M. Fazli, M. Eskandarian, Kinetic study for photocatalytic degradation of Direct Red 23 in UV–LED/nano-$TiO_2/S_2O_8^{2-}$ process: dependence of degradation kinetic on operational parameters, J. Ind. Eng. Chem., 20 (2014) 3695–3702.

[14] M.L. Satuf, M.J. Pierrestegui, L. Rossini, R.J. Brandi, O.M. Alfano, Kinetic modeling of azo dyes photocatalytic degradation in aqueous TiO_2 suspensions, toxicity and biodegradability evaluation, Catal. Today, 161 (2011) 121–126.

[15] S.L. Butterworth, Granular activated carbon as a toxicity reduction technology for wastewater treatment, Proc. Am. Chem. Soc. Spring Natl. Meet. Fuel Chem. Div., 41 (1996) 466–471.

[16] H. Zangeneh, A.A.L. Zinatizadeh, M. Habibi, M. Akia, M.H. Isa, Photocatalytic oxidation of organic dyes and pollutants in wastewater using different modified titanium dioxides: a comparative review, J. Ind. Eng. Chem., 26 (2015) 1–36.

[17] L. Zhao, X.Y. Hu, B.Y. Chen, C.C. Hsueh, Q. Zhang, J. Wang, Y.J. Lin, C.T. Chang, Synthesized TiO_2/ZSM-5 composites used for the photocatalytic degradation of azo dye: intermediates, reaction pathway, mechanism and bio-toxicity, Appl. Surf. Sci., 383 (2016) 300–309.

[18] D. Chebli, F. Fourcade, S. Brosillon, S. Nacef, A. Amrane, Supported photocatalysis as a pre-treatment prior to biological degradation for the removal of some dyes from aqueous solutions; Acid Red 183, Biebrich Scarlet, Methyl Red Sodium Salt, Orange II, J. Chem. Technol. Biotechnol., 85 (2010) 555–563.

[19] S. Hisaindee, M.A. Meetani, M.A. Rauf, Application of LC-MS to the analysis of advanced oxidation process (AOP) degradation of dye products and reaction mechanisms, TrAC, Trends Anal. Chem., 49 (2013) 31–44.

[20] D. Gunjan, B. Gargi, Toxicity tests to check water quality, Int. Res. J. Environ. Sci., 4 (2015) 87–90.

[21] Y. Luo, J. Liang, G. Zeng, M. Chen, D. Mo, G. Li, D. Zhang, Seed germination test for toxicity evaluation of compost: its roles, problems and prospects, Waste Manage., 71 (2018) 109–114.

[22] K.A. Gyekye, An assessment of toxic in urban soils using garden cress (*Lepidium sativum*) in Vasileostrovsky Ostrov and Elagin Ostrov, Saint Petersburg, Russia, J. Geogr. Geol., 5 (2013) 63–70.

[23] S. Khezrianjoo, H.D. Revanasiddappa, Evaluation of kinetics and energy consumption of the electrochemical oxidation of Acid Red 73 in aqueous media, Toxicol. Environ. Chem., 98 (2016) 759–767.

[24] J. Saien, A.R. Soleymani, Degradation and mineralization of Direct Blue 71 in a circulating upflow reactor by UV/TiO_2 process and employing a new method in kinetic study, J. Hazard. Mater., 144 (2007) 506–512.

[25] N.M. Mahmoodi, M. Arami, Degradation and toxicity reduction of textile wastewater using immobilized titania nanophotocatalysis, J. Photochem. Photobiol. B, 94 (2009) 20–24.

[26] I. Arslan-Alaton, Degradation of a commercial textile biocide with advanced oxidation processes and ozone, J. Environ. Manage., 82 (2007) 145–154.

[27] G. Lencioni, D. Imperiale, N. Cavirani, N. Marmiroli, M. Marmiroli, Environmental application and phytotoxicity of anaerobic digestate from pig farming by in vitro and in vivo trials, Int. J. Environ. Sci. Technol., 13 (2016) 2549–2560.

[28] R.A. Nastro, A. Suglia, V. Pasquale, M. Toscanesi, M. Trifuoggi, M. Guida, Efficiency measures of polycyclic aromatic hydrocarbons bioremediation process through ecotoxicological tests, Int. J. Perform. Eng., 10 (2014) 411–418.

[29] E.W. Rice, L. Bridgewater, Standard methods for the examination of water and wastewater, 22nd, American Water Works Association, Washington, D.C., 2012.

[30] S. Khezrianjoo, H.D. Revanasiddappa, Effect of operational parameters and kinetic study on the photocatalytic degradation of *m*-cresol purple using irradiated ZnO in aqueous medium, Water Qual. Res. J. Can., 51 (2016) 69–78.

[31] H. Rezaei-Vahidian, A.R. Zarei, A.R. Soleymani, Degradation of nitro-aromatic explosives using recyclable magnetic photocatalyst: catalyst synthesis and process optimization, J. Hazard. Mater., 325 (2017) 310–318.

[32] I.K. Konstantinou, T.A. Albanis, TiO_2-assisted photocatalytic degradation of azo dyes in aqueous solution: kinetic and mechanistic investigations: a review, Appl. Catal. B, 49 (2004) 1–14.

[33] A.S. González, S.S. Martínez, Study of the sonophotocatalytic degradation of basic blue 9 industrial textile dye over slurry titanium dioxide and influencing factors, Ultrason. Sonochem., 15 (2008) 1038–1042.

[34] J. Saien, S. Khezrianjoo, Degradation of the fungicide Carbendazim in aqueous solutions with UV/TiO_2 process: optimization, kinetics and toxicity studies, J. Hazard. Mater., 157 (2008) 269–276.

[35] J. Saien, A.R. Soleymani, Comparative investigations on nano and micro titania photocatalysts in degradation and mineralization: use of turbidity in kinetic studies, J. Iran. Chem. Soc., 6 (2009) 602–611.

[36] J. Saien, H. Nejati, Enhanced photocatalytic degradation of pollutants in petroleum refinery wastewater under mild conditions, J. Hazard. Mater., 148 (2007) 491–495.

[37] D. Mantzavinos, E. Psillakis, Enhancement of biodegradability of industrial wastewaters by chemical oxidation pre-treatment, J. Chem. Technol. Biotechnol., 79 (2004) 431–454.

[38] L. Zhao, B. Zhang, X. Xiao, F.L. Gu, Roles of the active species involved in the photocatalytic oxidation of benzyl alcohol into benzaldehyde on TiO_2 under UV light: experimental and DFT studies, J. Mol. Catal. A Chem., 420 (2016) 82–87.

[39] W. Li, D. Li, Y. Lin, P. Wang, W. Chen, X. Fu, Y. Shao, Evidence for the active species involved in the photodegradation process of Methyl Orange on TiO_2, J. Phys. Chem. C, 116 (2012) 3552–3560.

[40] P.F. Schwarz, N.J. Turro, S.H. Bossmann, A.M. Braun, A.M.A.A. Wahab, H. Durr, A new method to determine the generation of hydroxyl radicals in illuminated TiO_2 suspensions, J. Phys. Chem. B, 101 (1997) 7127–7134.

[41] Y. Nosaka, A. Nosaka, Understanding hydroxyl radical ($^{\bullet}$OH) generation processes in photocatalysis, ACS Energy Lett., 1 (2016) 356–359.

[42] S. Zhou, A.K. Ray, Kinetic studies for photocatalytic degradation of Eosin B on a thin film of titanium dioxide, Ind. Eng. Chem. Res., 42 (2003) 6020–6033.

[43] F. Shahrezaei, Y. Mansouri, A.A.L. Zinatizadeh, A. Akhbari, Photocatalytic degradation of Aniline using nanoparticles in a vertical circulating photocatalytic reactor, Int. J. Photoenergy, 2012 (2012) 1–8.

[44] S. Khezrianjoo, H.D. Revanasiddappa, Langmuir-Hinshelwood kinetic expression for the photocatalytic degradation of Metanil Yellow aqueous solutions by ZnO catalyst, Chem. Sci. J., 2012 (2012) 1–7.

[45] M.F. Atitar, A. Bouziani, R. Dillert, M.E. Azzouzi, D.W. Bahnemann, Photocatalytic degradation of the herbicide imazapyr: do the initial degradation rates correlate with the adsorption kinetics and isotherms? Catal. Sci. Technol., 8 (2018) 985–995.

[46] S. Papic, I. Peternel, Z. Krevzelj, H. Kusic, N. Koprivanac, Advanced oxidation of an azo dye and its synthesis intermediates in aqueous solution: effect of fenton treatment on mineralization, biodegradability and toxicity, Environ. Eng. Manage. J., 13 (2014) 2561–2571.

[47] B. Alexander, D.J. Browse, S.J. Reading, I.S. Benjamin, A simple and accurate mathematical method for calculation of the EC_{50}, J. Pharmacol. Toxicol. Methods, 41 (1999) 55–58.

[48] P. Thomas, N. Soren, N.P. Rumjit, J. George James, M.P. Saravanakumar, Biomass resources and potential of anaerobic digestion in Indian scenario, Renewable Sustainable Energy Rev., 77 (2017) 718–730.

Supplementary information

Further information on constructed photo-reactor

As it can be seen in Fig. S1, the UV lamp was positioned centrally in the constructed reactor inside the quartz tube. The lamp was totally covered by DY11 solution; therefore, maximum light utilization was achieved and no dead space was in the reactor. To reduce the absorption of light photons by oxygen molecules in the air around the lamp, diameter of the quartz tube was minimized. The pump has been received the solution from top of the reactor and delivered it to the bottom; this was provided an up-flow and adjustable batch circulating system with no catalyst separation. The circulating pump had a flow-rate of about 5200 (mL/min); so, both fluidizing and the well mixing of catalyst particles around the quartz tube has been provided. For regulating the solution temperature, the reactor has been equipped with a water-flow jacket by means of an external circulating flow; a thermostat bath (OPTIMA-740, Japan) with an accuracy of ±0.1°C was used for adjustment of external circulating water flow temperature. Since the photocatalytic oxidation process is sustained by the ready supply of dissolved oxygen, the air was blown into the solution using an air compressor (RS-510).

UV-Vis spectra analysis as well as image of germination and root growth of LSL

DY11 is a mono azo dye in which the strong absorbance in the visible region (404 nm) is related to the chromophore part of molecular structure (azo linkage), while the absorbance peaks of the naphthalene and benzene rings are appeared in the UV region (about 250 nm). Full spectra scanning of the target dye was followed during the time-course of PCO process (Fig. S3). A gradual disappearance of the absorbance peaks around 404 nm that observed during the time-course showed almost perfect degradation of the main chromophores. Therefore, nearly complete decolorization (95%) was achieved in the presence of TiO_2 suspension after 120 min. It has been reported that the intensity of the azo band (visible light chromophore) decreases with time more rapidly than the chromophore of aromatic rings [18]. The slower decrease of the previous chromophores could be due to the formation of byproducts which contain aromatic rings before the opening of them. In the current study the absorbance peaks at UV region (around 250 nm) was increased in first 60 min of illumination due to the generation of aromatic intermediates and decreased moderately after this time.

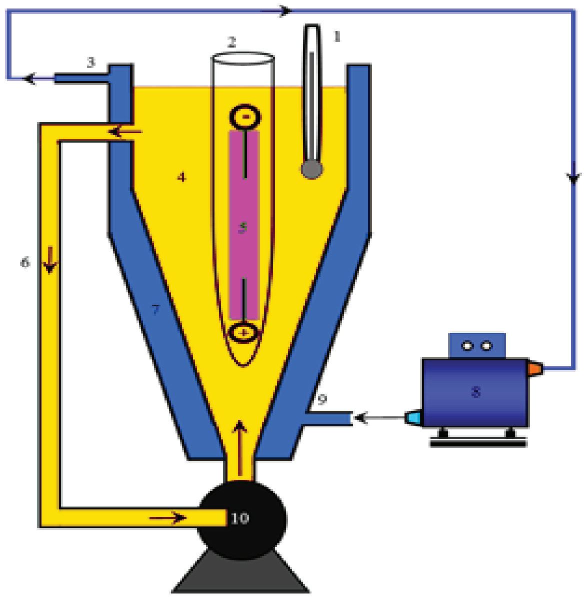

Fig. S1. The scheme view of photo-reactor: 1 - thermometer, 2 - quartz tube, 3 - external circulating water flow outlet (for adjustment of temperature), 4 - DY11 solution, 5 - UV lamp, 6 - recycling stream, 7 - water-flow jacket, 8 - thermostat, 9 - external water flow inlet, 10 - pump.

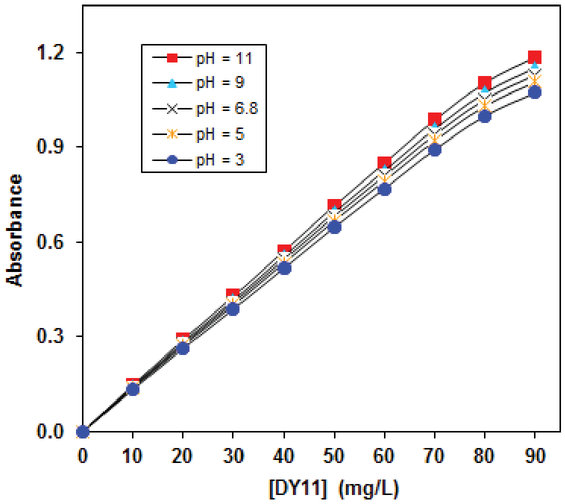

Fig. S2. The calibration chart for measuring DY11 concentration at different pH values; T = 25°C.

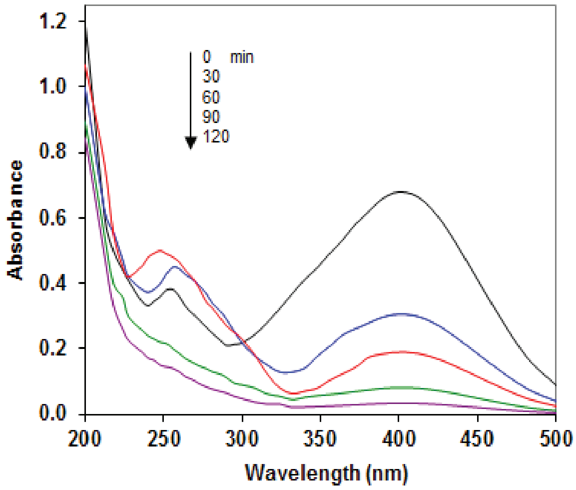

Fig. S3. UV–Vis spectra changes of DY11 at different irradiation times; $[DY11]_0$ = 50 mg/L, $[TiO_2]$ = 90 mg/L, T = 25°C and pH 6.8 (natural).

As it can be seen in Fig. S4, after 60 min of irradiation number of *LSL* germinated seeds as well as its root length was decreased. Thus, the toxic properties of solution (number and/or concentration of toxic intermediates) have been increased in this period. For illumination times longer than 60 min, the number of *LSL* germinated seeds as well as its root length tended to increase as result of decrease in solution toxicity.

Further information on investigation on active species

Due to the extremely high rate constant of reaction between hydroxyl radicals and ethanol (1.9 × 10^9 1/Ms), this alcohol could be used to quench hydroxyl radicals [35]. Consequently, PCO of DY11 with initial concentration of 50 mg/L were performed using different amount of catalyst (30, 60 and 90 mg/L), each of them with different amounts of added ethanol under natural pH (6.8) and ambient temperature (25°C); Fig. S5 present these results respectively. Adding small amount of ethanol to the dye solution until 0.1, 0.12 and 0.16 volumetric percentages (v/v) for catalyst concentration of 30, 60 and 90 (mg/L) has led to a decrease in degradation efficiency. The observed reduction by adding ethanol up to the certain percentage is due to the quench of hydroxyl radicals by the ethanol molecules and therefore can be introduced as the role of hydroxyl radicals in the process. On the other hand, adding extra amounts of ethanol causes the degradation efficiency to increase slightly. The formation of ethoxy radicals ($C_2H_5O^\bullet$) from direct PCO of ethanol can help in this regard. Meanwhile, the ethanol molecules would generate the hydroxyl radicals in direct photolysis with respect to the level of C–O energy bond [35].

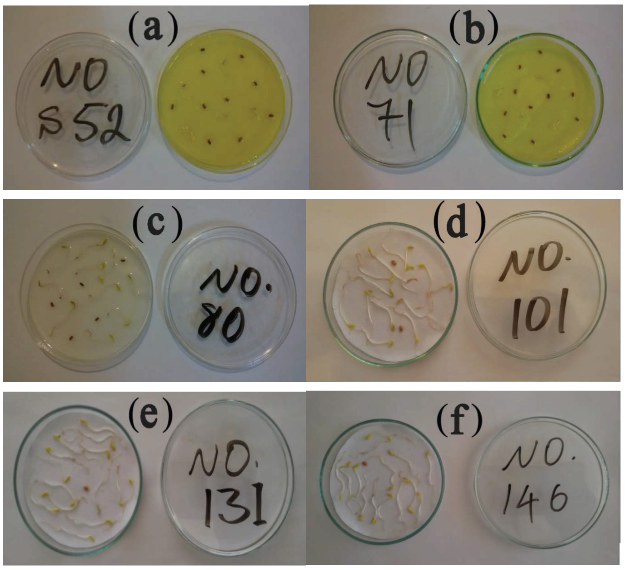

Fig. S4. Root growth and seed germination percentage of *LSL* in DY11 solution during the PCO process; $[DY11]_0$ = 50 mg/L, $[TiO_2]$ = 90 mg/L, T = 25°C and pH 6.8 (natural). (a): before illumination, (b): after 60 min of illumination, (c): after 120 min of illumination, (d): after 180 min of illumination, (e): after 240 min of illumination and (f): after 300 min of illumination.

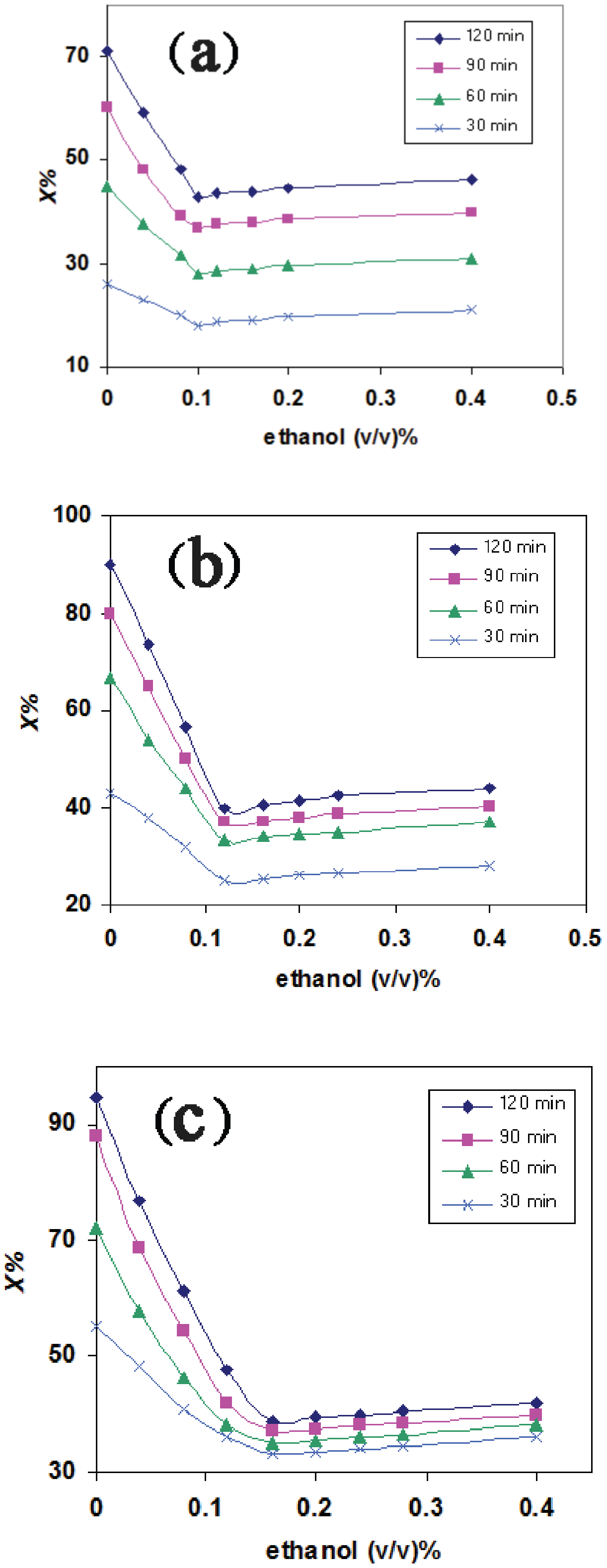

Fig. S5. Variation of the degradation of DY11 in PCO process versus added amounts of ethanol at different catalyst concentrations and irradiation times; $[DY11]_0$ = 50 mg/L, T = 25°C and pH = 6.8 (natural). (a): $[TiO_2]$ = 30 mg/L, (b): $[TiO_2]$ = 60 mg/L and (c): $[TiO_2]$ = 90 mg/L.

Table S1
Pseudo-first-order kinetic rate constants for the photocatalytic degradation of DY11 at pH values of 5, 6.8 and 9 with different initial concentrations; $[TiO_2]$ = 90 mg/L and T = 25°C.

$[DY11]_0$ (mg/L)	10	20	30	40	50
$k_{obs}\times10^2$ (1/min) pH = 5	6.75	4.29	2.94	2.45	1.92
$k_{obs}\times10^2$ (1/min) pH = 6.8	9.81	5.71	3.92	2.88	2.41
$k_{obs}\times10^2$ (1/min) pH = 9	14.90	6.91	5.09	4.11	2.97

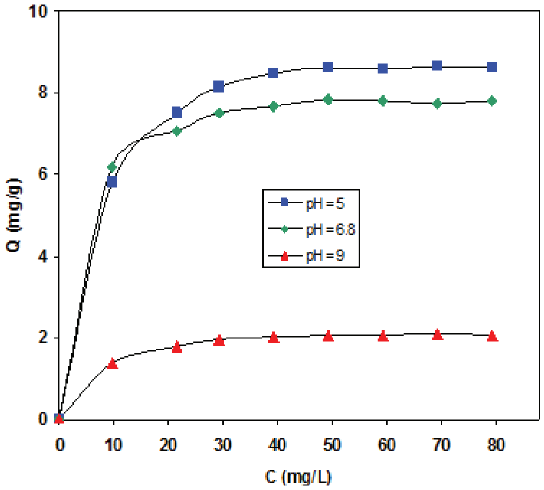

Fig. S6. Adsorption isotherm of DY11 on TiO_2 in different pH values, quantity adsorbed as a function of equilibrium concentration; $[TiO_2]$ = 90 mg/L and T = 25°C.

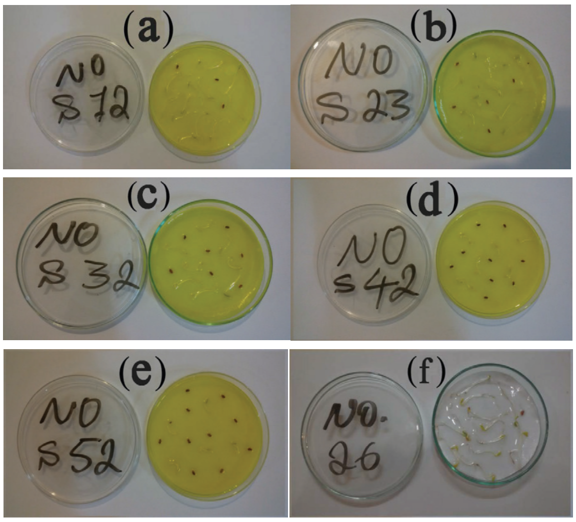

Fig. S7. Effect of different concentrations of DY11 that induce inhibition on *LSL* root growth and seed germination percentage; T = 25°C. (a): [DY11] = 10 mg/L, (b): [DY11] = 20 mg/L, (c): [DY11] = 30 mg/L, (d): [DY11] = 40 mg/L, (e): [DY11] = 50 mg/L and (f): Control (distilled water).

Details about the adsorption equilibrium constant

As it can be seen in Fig. S6, in the examined pH values of 5, 6.8 and 9, adsorption of dye on catalyst surface increases with the initial concentration of DY11 to about 50 mg/L and then finds a tendency toward independent values with the higher initial concentrations. This plateau corresponded to attainment of limiting solubility for solute in the solution monolayer [44].